Cell Metabolism, Volume *29*

Supplemental Information

Transcriptional Basis for Rhythmic Control of Hunger and Metabolism within the AgRP Neuron

Jonathan Cedernaes, Wenyu Huang, Kathryn Moynihan Ramsey, Nathan Waldeck, Lei Cheng, Biliana Marcheva, Chiaki Omura, Yumiko Kobayashi, Clara Bien Peek, Daniel C. Levine, Ravindra Dhir, Raj Awatramani, Christopher A. Bradfield, Xiaozhong A. Wang, Joseph S. Takahashi, Mohamad Mokadem, Rexford S. Ahima, and Joseph Bass

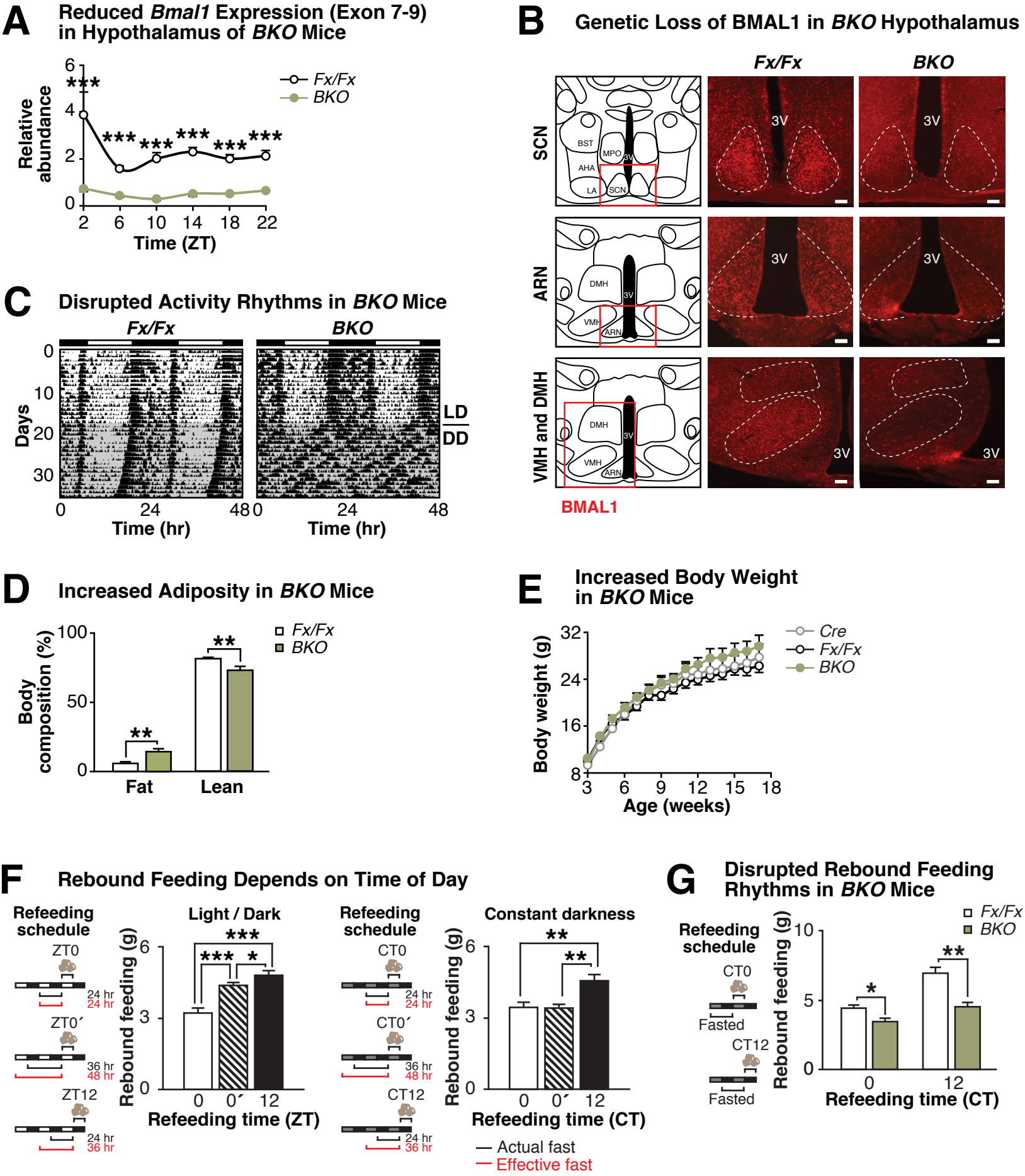
A
Reduced Bmal1 Expression (Exon 7-9) in Hypothalamus of BKO Mice
Relative abundance
Fx/Fx
BKO
Time (ZT)
B
Genetic Loss of BMAL1 in BKO Hypothalamus
Fx/Fx
BKO
SCN
ARN
VMH and DMH
BST
MPO
AHA
LA
SCN
DMH
VMH
ARN
3V
BMAL1
C
Disrupted Activity Rhythms in BKO Mice
Fx/Fx
BKO
Days
LD
DD
Time (hr)
D
Increased Adiposity in BKO Mice
Body composition (%)
Fx/Fx
BKO
Fat
Lean
E
Increased Body Weight in BKO Mice
Body weight (g)
Cre
Fx/Fx
BKO
Age (weeks)
F
Rebound Feeding Depends on Time of Day
Refeeding schedule
ZT0
ZT0′
ZT12
24 hr
36 hr
48 hr
Light / Dark
Rebound feeding (g)
Refeeding time (ZT)
CT0
CT0′
CT12
Constant darkness
Refeeding time (CT)
Actual fast
Effective fast
G
Disrupted Rebound Feeding Rhythms in BKO Mice
Refeeding schedule
CT0
Fasted
CT12
Rebound feeding (g)
Fx/Fx
BKO
Refeeding time (CT)

Figure S1. Genetic ablation of BMAL1 in hypothalamus impacts adiposity and time-of-day-dependent hunger. Related to Figure 1. (A) Relative abundance of mRNA (by qPCR) encoding the targeted *Bmal1* exon in mediobasal hypothalami of *Bmal1*$^{fx/fx}$ (white) and *BKO* (green) mice (n=3-4). **(B)** BMAL1 expression (red) in neurons of the suprachiasmatic nucleus (SCN, arcuate nucleus (ARN), ventromedial hypothalamus (VMH), and dorsomedial hypothalamus (DMH) (outlined in white dotted lines), as assessed by immunohistochemistry. Scale bar represents 100 μm. **(C)** Representative actograms from *Bmal1*$^{fx/fx}$ and *BKO* mice. Activity counts are indicated by vertical black marks in the activity record. The records are double-plotted so that each day's record is presented on both left and right, and beneath that of the previous day. Mice were maintained on a 12:12 LD schedule for 18 days prior to being transferred to constant darkness (DD) on the day indicated by a horizontal line in the margin. **(D)** Body composition (fat and lean mass) (n=7-8) and **(E)** body weight trajectory in *ad lib*-fed *Bmal1*$^{fx/fx}$, *Camk2α-Cre*, and *BKO* mice; *BKO* mice were significantly heavier than both the *Camk2α-Cre* ($p<0.04$) and *Fx/Fx* ($p<0.001$) mice by Tukey's multiple comparison test (n=2-11). **(F)** Amount of rebound feeding (i.e., food intake in the 12 hrs after re-introduction of food following a fast) in wild-type (WT) mice when refeeding starts at ZT0 (i.e., lights on) following either a 24-h fast (white) or an extended 36-h fast (striped) or at ZT12 (i.e., lights off) following a 24-h fast (black) (n=8). The refeeding schedule on the left highlights the researcher-imposed fasting ("actual fast"), as well as the "effective fast", i.e., the fact that mice will primarily be fasting during preceding *ad lib* light periods. Comparable rebound feeding in WT mice held in constant darkness (DD) is shown on the right (n=5). **(G)** Amount of rebound feeding in *Bmal1*$^{fx/fx}$ and *BKO* mice following refeeding in constant darkness (DD) at CT0 and CT12 (n=4-5). Data are represented as mean ± SEM (*$p<0.05$, **$p<0.01$, ***$p<0.001$).

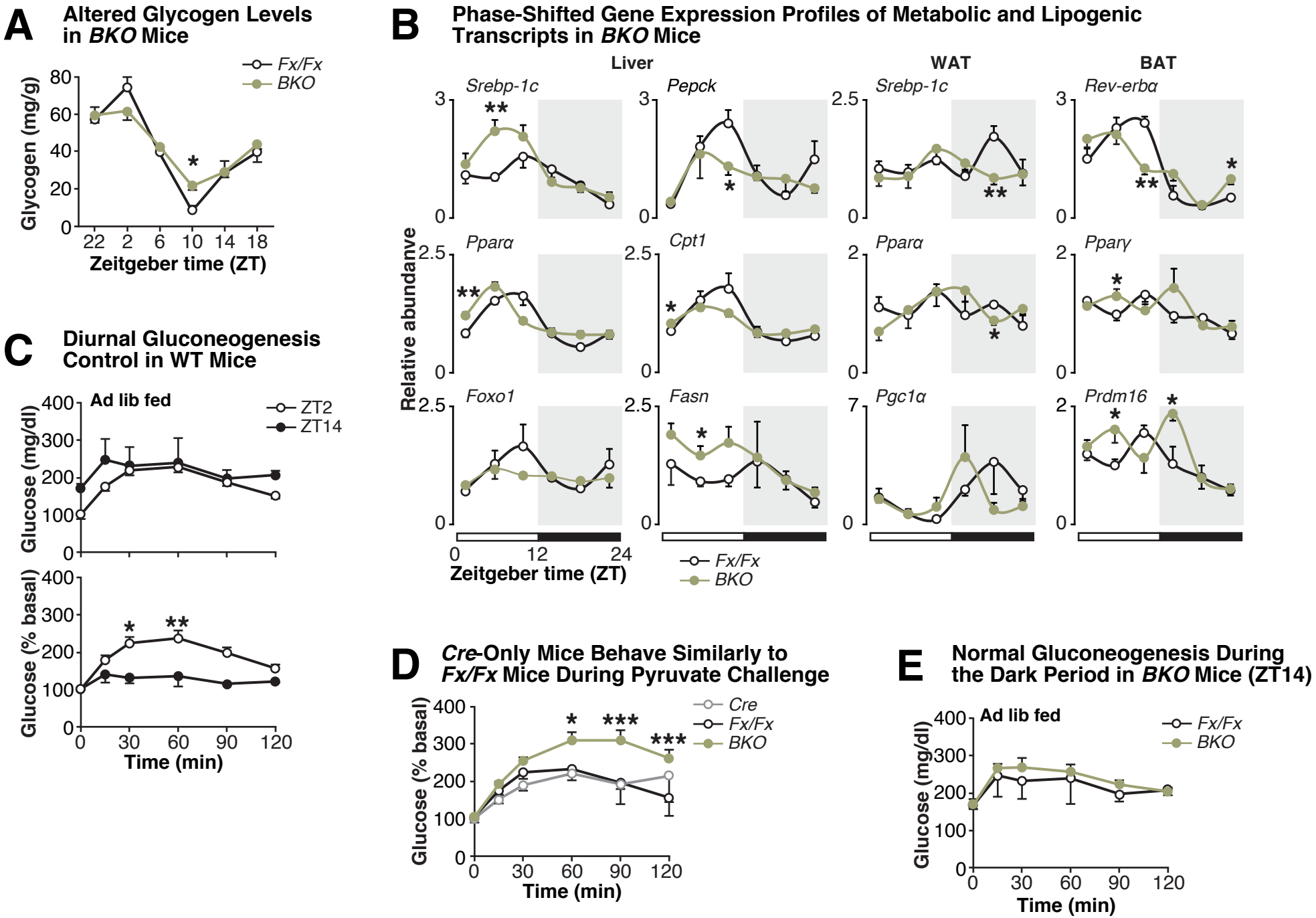
A
Altered Glycogen Levels in BKO Mice
Fx/Fx
BKO
Glycogen (mg/g)
Zeitgeber time (ZT)
B
Phase-Shifted Gene Expression Profiles of Metabolic and Lipogenic Transcripts in BKO Mice
Liver
WAT
BAT
Srebp-1c
Pepck
Srebp-1c
Rev-erbα
Pparα
Cpt1
Pparα
Pparγ
Foxo1
Fasn
Pgc1α
Prdm16
Relative abundanve
Zeitgeber time (ZT)
Fx/Fx
BKO
C
Diurnal Gluconeogenesis Control in WT Mice
Ad lib fed
ZT2
ZT14
Glucose (mg/dl)
Glucose (% basal)
Time (min)
D
Cre-Only Mice Behave Similarly to Fx/Fx Mice During Pyruvate Challenge
Cre
Fx/Fx
BKO
Glucose (% basal)
Time (min)
E
Normal Gluconeogenesis During the Dark Period in BKO Mice (ZT14)
Ad lib fed
Fx/Fx
BKO
Glucose (mg/dl)
Time (min)

Figure S2. Neuronal clock regulates time-of-day-dependent metabolism. Related to Figure 1. (A) 24-h glycogen levels (n=3-4) in *Bmal1*$^{fx/fx}$ and *BKO* mice. **(B)** 24-h mRNA expression of metabolic transcription factors and lipogenic and gluconeogenic genes in *ad lib*-fed *Bmal1*$^{fx/fx}$ and *BKO* mice in liver, white adipose tissue (WAT), and brown adipose tissue (BAT) (n=3-4). **(C-E)** Time course of plasma glucose levels following an intraperitoneal injection of pyruvate (2 mg/kg) in **(C)** fasted WT mice at ZT2 (open circles) and ZT14 (closed circles) (n=3-10) (left panel: absolute glucose values, ANOVA time effect p=0.0035; right panel: fold change from pre-injection baseline, ANOVA ZT2 vs ZT14 effect: p<0.0001); **(D)** fasted *Bmal1*$^{fx/fx}$, *Camk2α-Cre*, and *BKO* mice at ZT2 (n=2-14) (*BKO* vs. *Bmal1*$^{fx/fx}$: ANOVA genotype effect: p<0.0001; post-hoc *BKO* vs. *Bmal1*$^{fx/fx}$ differences at indicated timepoints) and **(E)** fasted *Bmal1*$^{fx/fx}$ and *BKO* mice at ZT14 (n=7) (ANOVA genotype effect: p=0.31). Data are represented as mean ± SEM (*p<0.05, **p<0.01, ***p<0.001).

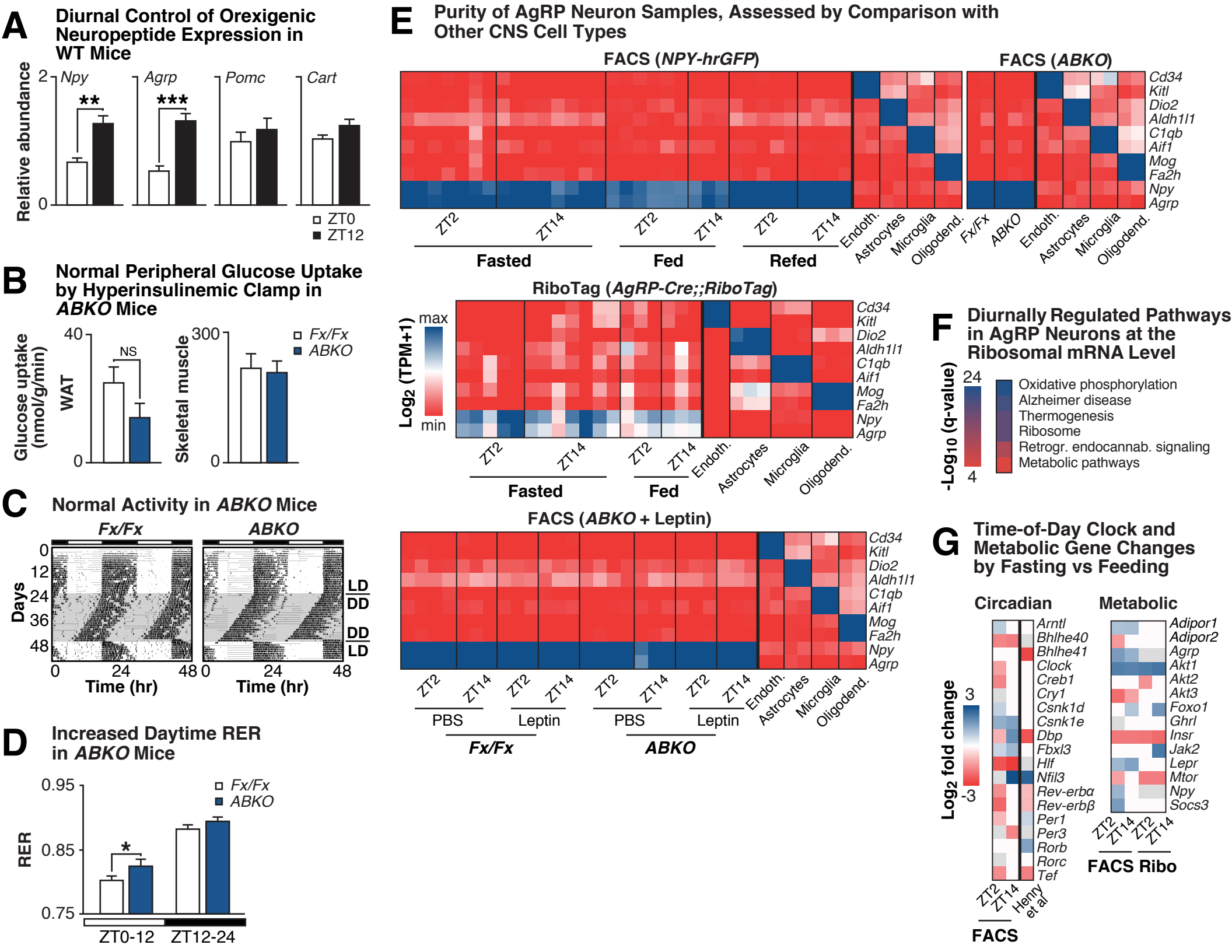
A
Diurnal Control of Orexigenic Neuropeptide Expression in WT Mice
Relative abundance
Npy
Agrp
Pomc
Cart
**
***
ZT0
ZT12
B
Normal Peripheral Glucose Uptake by Hyperinsulinemic Clamp in ABKO Mice
Glucose uptake (nmol/g/min)
WAT
Skeletal muscle
NS
Fx/Fx
ABKO
C
Normal Activity in ABKO Mice
Fx/Fx
ABKO
Days
LD
DD
DD
LD
Time (hr)
Time (hr)
D
Increased Daytime RER in ABKO Mice
RER
Fx/Fx
ABKO
*
ZT0-12
ZT12-24
E
Purity of AgRP Neuron Samples, Assessed by Comparison with Other CNS Cell Types
FACS (NPY-hrGFP)
FACS (ABKO)
Cd34
Kitl
Dio2
Aldh1l1
C1qb
Aif1
Mog
Fa2h
Npy
Agrp
ZT2
ZT14
Fasted
Fed
Refed
Endoth.
Astrocytes
Microglia
Oligodend.
Fx/Fx
ABKO
RiboTag (AgRP-Cre;;RiboTag)
Log2 (TPM+1)
max
min
FACS (ABKO + Leptin)
PBS
Leptin
Fx/Fx
ABKO
F
Diurnally Regulated Pathways in AgRP Neurons at the Ribosomal mRNA Level
-Log10 (q-value)
Oxidative phosphorylation
Alzheimer disease
Thermogenesis
Ribosome
Retrogr. endocannab. signaling
Metabolic pathways
G
Time-of-Day Clock and Metabolic Gene Changes by Fasting vs Feeding
Circadian
Metabolic
Log2 fold change
Arntl
Bhlhe40
Bhlhe41
Clock
Creb1
Cry1
Csnk1d
Csnk1e
Dbp
Fbxl3
Hlf
Nfil3
Rev-erbα
Rev-erbβ
Per1
Per3
Rorb
Rorc
Tef
Adipor1
Adipor2
Agrp
Akt1
Akt2
Akt3
Foxo1
Ghrl
Insr
Jak2
Lepr
Mtor
Npy
Socs3
FACS
Henry et al
FACS
Ribo

Figure S3. Loss of clock in AgRP neurons leads to increased food consumption, RER, and body weight, and FACS and RiboTag samples show enrichment of neuron-specific markers. Related to Figures 2-4. (A) mRNA expression of neuropeptides in WT mice fasted for 24 h and collected at the onset of either the light (ZT0) or dark (ZT12) period (n=7). **(B)** Glucose uptake in WAT (p=0.15, two-tailed unpaired student's t-test) and skeletal muscle as assessed by hyperinsulinemic clamp in *Bmal1*$^{fx/fx}$ and *ABKO* mice (n=5-9). **(C)** Double-plotted locomotor activity (based on wheel activity) in *Bmal1*$^{fx/fx}$ and *ABKO* mice, under normal (12:12) light/dark conditions (LD), as well as under constant darkness (DD) (n=6-8). **(D)** Respiratory exchange ratio (RER) values (VCO_2/VO_2) in the light (ZT0-12) and dark (ZT12-24) period in *Bmal1*$^{fx/fx}$ and *ABKO* mice (n=5-7) (ANOVA, ZT0-24, genotype effect, p=0.0145, Sidak's multiple comparison test ZT0-12, p=0.0482, ZT12-24: p=0.35). Data are represented as mean ± SEM (*p<0.05, **p<0.01, ***p<0.001). (**E**) Purity of individual FACS and RiboTag samples in Figures 2-4, as assessed by comparison with previously published cell type-specific FACS data from endothelial cells, astrocytes, microglia, and oligodendrocytes (Avey et al., 2018; Haimon et al., 2018; Sun et al., 2017; Zhang et al., 2014). Showing enriched markers at the maximum transcripts per million (TPM; log_2-transformed) per cell type for indicated conditions for both FACS and RiboTag samples. (**F**) KEGG pathways that were significantly enriched (FDR<0.05) in analyses of *AgRP-Cre;;RiboTag* mice fasted at ZT2 versus ZT14. (**G**) Changes in circadian clock genes in response to fasting versus *ad lib* feeding in *NPY-hrGFP* mice at ZT2 and ZT14. Also shows the corresponding data from AgRP neurons from (Henry et al., 2015).

A Transcription Factor Motifs Induced by Fasting vs Feeding at the Whole Cell and Ribosome Level at Morning and Evening

FACS (*NPY-hrGFP*), ZT2

Consensus seq.	Motif	Q-val
	SP1	0.0000
	KLF3	0.0000
	RONIN	0.0001
	GFY-STAF	0.0002
	SP5	0.0002
	GFY	0.0004
	USF2	0.0005
	E-BOX	0.0027
	bHLHE40	0.0042
	KLF14	0.0062
	TFE3	0.0070
	ZNF143	0.0147
	ELK4	0.0147
	TGIF2	0.0153
	NFY	0.0175
	ELK1	0.0190
	USF1	0.0451
	KLF6	0.0451
	MAZ	0.0451
	YY1	0.0451

RiboTag (*AgRP-Cre;;RiboTag*), ZT2

Consensus seq.	Motif	Q-val
	ELK4	0.0000
	ELK1	0.0000
	FLI1	0.0000
	GABPA	0.0000
	ETV1	0.0002
	ELF1	0.0003
	ETS1	0.0003
	SP1	0.0005
	ETS	0.0012
	YY1	0.0028
	NFY	0.0197
	HOXD13	0.0252
	SP5	0.0322
	ETV2	0.0391
	PBX3	0.0468

RiboTag (*AgRP-Cre;;RiboTag*), ZT14

Consensus seq.	Motif	Q-val
	SP1	0.0438

FACS (*NPY-hrGFP*), ZT14

Consensus seq.	Motif	Q-val
	PKNOX1	0.0622
	PBX3	0.0622

B Transcription Factor Motifs Induced by Refeeding vs Fasting at the Whole Cell Level at Morning and Evening

FACS (*NPY-hrGFP*), ZT2

Consensus seq.	Motif	Q-val
	GFY-STAF	0.0233
	RONIN	0.0233
	SP1	0.0233
	GFY	0.0284

FACS (*NPY-hrGFP*), ZT14

Consensus seq.	Motif	Q-val
	PKNOX1	0.3124
	PBX3	0.3127
	SP1	0.3127

C Altered Leptin Rhythms in *BKO* Mice

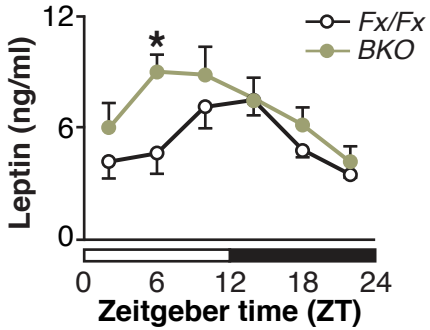

D Time-of-Day Dependent Differences in Leptin Levels After Fasting in WT Mice

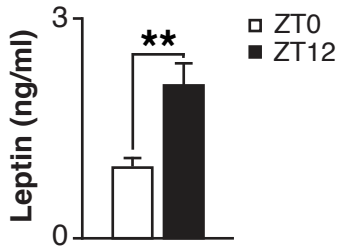

E Time-of-Day Dependent Differences in Leptin Sensitivity in WT Mice

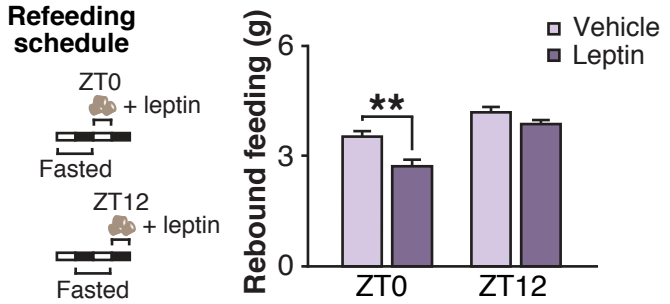

F Time-of-Day Dependent Differences in Phosphorylation of STAT3 in WT Mice

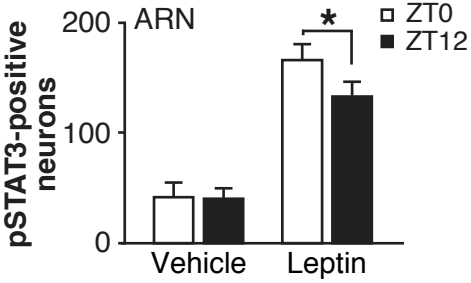

G Time-of-Day and Clock Dependent Transcriptional Response to Leptin in AgRP Neurons

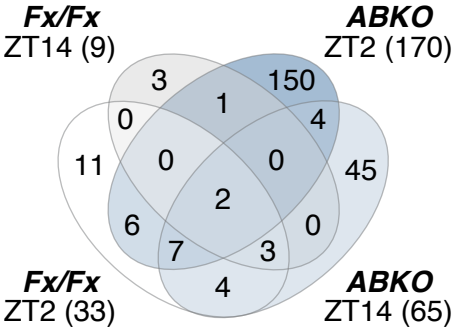

Figure S4. Transcription factor (TF) motif analysis reveals enrichment of nutrient-responsive TFs related to mitochondrial function, and *BKO* mice display altered leptin sensitivity. Related to Figures 3-4. TF motif analyses reveal significantly enriched consensus sequences and their associated TFs, both in **(A)** FACS and RiboTag analyses at ZT2 and ZT14 in fasted versus feeding and **(B)** FACS analyses at ZT2 and ZT14 following time-restricted feeding. **(C)** Leptin levels measured every 4 h in *ad lib*-fed *Bmal1*$^{fx/fx}$ and *BKO* mice (n=3-5). **(D)** Leptin levels in WT mice at either ZT0 or ZT12 following a 24-h fast (n=5-7). **(E)** Amount of rebound feeding (g) in WT mice following a 24-h fast when refeeding (measured over 11 hours) starts at either ZT0 (left bars) or ZT12 (right bars), at the same time that either vehicle or leptin (10 mg/kg) is injected (n=7-8). **(F)** pSTAT3-positive neurons at ZT0 versus ZT12 following either vehicle or leptin administration in the arcuate nucleus (n=5-6). **(G)** Venn diagram indicating numbers of genes whose expression changed due to either time of day (ZT2 versus 14) or genotype (*Bmal1*$^{fx/fx}$ versus *ABKO* mice) in response to acute leptin (2 mg/kg) administration. Data are represented as mean ± SEM (*$p<0.05$, **$p<0.01$).